Chemical Engineering Journal 159 (2010) 264–271

Contents lists available at ScienceDirect

Chemical Engineering Journal

journal homepage: www.elsevier.com/locate/cej

Efficient separation of heavy metal cations by anchoring polyacrylic acid on superparamagnetic magnetite nanoparticles through surface modification

Ali Reza Mahdavian[a,*], Monir Al-Sadat Mirrahimi[b]

[a] Polymer Science Department, Iran Polymer & Petrochemical Institute, P.O. Box 14965/115, Tehran, Iran
[b] Department of Chemistry, Faculty of Science Imam Khomeini International University, P.O. Box 34149-16818, Qazvin, Iran

ARTICLE INFO

Article history:
Received 8 September 2009
Received in revised form 9 February 2010
Accepted 20 February 2010

Keywords:
Polyelectrolytes
Magnetite
Superparamagnetic
Cation adsorption
Surface modification

ABSTRACT

Magnetite nanoparticles are an exceptional adsorbent materials due to their magnetic properties and good adsorption capacity. The aim of this work is to investigate the suitability of magnetite nanoparticles for adsorption of heavy metal cation and its efficiency. Magnetic iron oxide nanoparticles were successfully prepared by a coprecipitation method followed by modification with 3-aminopropyl triethoxysilane (APTES) and acryloyl chloride (AC) subsequently. Then the surface of modified nanoparticles was modified by graft polymerization with acrylic acid. The grafted magnetite nanoparticles were next used for separation of heavy metal cations. The adsorption of heavy metal cations from aqueous solution by polyacrylic acid grafted onto magnetite nanoparticles was studied too. The ability of heavy metal adsorption of these nanoparticles for removal from aqueous solutions was measured with atomic absorption technique and they showed their potential for the separation of heavy metal cations such as Cd^{2+}, Pb^{2+}, Ni^{2+} and Cu^{2+}. The obtained nanoparticles were characterized by X-ray diffraction (XRD), scanning electron microscopy (SEM), vibrating sample magnetometer (VSM), Fourier transform infrared (FT-IR), thermogravimetric analysis (TGA) and DSC analyses with the size ranging from 10 to 23 nm. The magnetite nanoparticles exhibited superparamagnetism above 300 K and the saturation magnetization was 57.1 emu/g at 300 K.

1. Introduction

In recent years, magnetic nanoparticles (MNPs) have gained an increasing interest because of their potential applications; examples include their uses for cell separation [1], magnetic resonance imaging [2], drug delivery systems [3], protein separation [4], and cancer treatments through hyperthermia [5]. The methods of surface modification for MNPs usually include adsorption or conjunction of polymers [6–9] and surface polymerization [10,11]. The magnetic part is often an inorganic magnetic nanoparticle, such as Fe_2O_3, Fe_3O_4, etc. The polymer part, such as polyethylene [12], polystyrene [13], starch [14], chitosan [15], etc. provides favourable function to magnetic particles.

Several methods have been developed to prepare polymer coatings on magnetite nanoparticles such as physical adsorption of polymers, emulsion polymerization in the presence of nanoparticles, and the so-called "grafting-to" and "grafting-from" methods [16–19].

In addition, the application of magnetic particle technology to solve environmental problems has received considerable attention in recent years. Magnetic particles can be used to adsorb contaminants from aqueous or gaseous effluents and, after adsorption, can be separated from the medium by a simple magnetic field. Examples of this technology are the use of magnetite particles to accelerate the coagulation of sewage [20], a magnetite-coated functionalized polymer to remove radionuclides from milk [21], poly(oxy-2,6-dimethyl-1,4-phenylene) for the adsorption of organic dyes [22] and polymer-coated magnetic particles for oil spill remediation [23]. Magnetic adsorbents can be used to adsorb contaminants from aqueous effluents. After adsorption, the adsorbents can be separated from the medium by a simple magnetic process [24]. Magnetic adsorbents are usually prepared by the functionalization of magnetic particles through organic vapour condensation, polymer coating, surfactant adsorption, and direct silylation with silane coupling agents [25–27].

One of the interesting application of magnetic adsorbents is in the fields of environmental engineering, bioseparation, and biomedicine. Examples for environmental applications include the use of activated carbon and clay magnetic composites for the adsorption of contaminants in water [28,29], poly(1-vinylimidazole)-grafted magnetic nanoparticles for the removal of metal ions [25], removal of aluminium by alizarin yellow-attached magnetic poly(2-hydroxyethyl methacrylate) beads [30], polyacrylic acid (PAA) [31] and magnetic particles for enzyme recovery [32]. With increasing industrial activities, wastewater from many industries such as tannery, chemical manufacturing,

* Corresponding author. Tel.: +98 21 4458 0000; fax: +98 21 4458 0023.
E-mail address: a.mahdavian@ippi.ac.ir (A.R. Mahdavian).

1385-8947/$ – see front matter © 2010 Elsevier B.V. All rights reserved.
doi:10.1016/j.cej.2010.02.041

mining, battery manufacturing industries, etc., contains toxic heavy metals, which are dangerous and tend to accumulate in the living organisms, causing various diseases and disorders. Chromium (Cr), copper (Cu), cadmium (Cd) and nickel (Ni) are listed in the 11 hazardous priority substances of pollutants [33]. Copper is the most important and frequently used metal in industries such as plating, mining and petroleum refining. The industries mentioned above produce a great amount of wastewater and sludge containing a high concentration of copper cations, which have negative effects on the environment and water [34]. Cadmium and solutions of its compounds are toxic and serious toxicity problems have been found from long-term exposure and work with cadmium plating baths. Finally, nickel sulphide fume and dust are recognized as having carcinogenic potential. At the same time, the market for Ni–Cd batteries has been growing significantly in recent years. It means that there is enhanced potential for an increasing content of Ni and/or Cd in water [35]. Nowadays, magnetically active polymeric particles and dual-zone sorbents have been prepared by dispersing magnetite nanoparticles within the polymer phase and examined for their performance in removing contaminants such as Cu, Zn, as ions and dichlorophenol [36].

Moeser et al. [37] prepared magnetite nanoparticles (~7.5 nm) coated with a bifunctional polymer layer (~9 nm in thickness), consisting of an outer hydrophilic polyethylene oxide region and an inner hydrophobic polypropylene oxide region. The nanoparticles showed a high affinity to various synthetic organic compounds (toluene, *o*-dichlorobenzene, and naphthalene, etc.) in contaminated water. However, the previous researches on magnetite nanoparticle synthesis utilized commercial or reagent-grade chemicals as the iron source. High raw chemical costs could limit the utilization of magnetite nanoparticles for full-scale environmental engineering processes, since water or wastewater treatment usually entails large volumes of flow with a heterogeneous mixture of pollutants. On the other hand, their remarkable separation efficiency and ease of work have caused them be a developing subject in recent years.

Iron oxide or Fe_3O_4 is ferrimagnetism (ferromagnetic). Ferrimagnetism is a property exhibited by materials whose atoms or ions tend to assume an ordered but non-parallel arrangement in zero applied fields below a certain characteristic temperature known as the Neel temperature (e.g., Fe_3O_4 and Fe_3S_4). Above the Neel temperature, the substance becomes paramagnetic. Size reduction in magnetic materials resulting in the formation of single-domain particles also gives rise to the phenomenon of superparamagnetism. Briefly, superparamagnetism occurs when thermal fluctuations or an applied field can easily move the magnetic moments of the nanoparticle away from the easy axis, the preferred crystallographic axes for the magnetic moment to point along [38].

The saturation magnetization (M_s) values found in nanostructured materials are usually smaller than the corresponding bulk phases, provided that no change in ionic configurations occurs. Accordingly, experimental values for M_s (i.e., magnetic saturation) in magnetite nanoparticles have been reported to span the 30–50 emu/g, lower than the bulk magnetite value; 90 emu/g [39]. Many studies have been reported on the origin of the observed reduction in magnetization in fine magnetic particles. Also, in magnetite fine particles, Varanda et al. [40] have reported a linear correlation between saturation magnetization and particle size, suggesting that defects at the particle surface can influence the magnetic properties. The surface curvature of the nanoparticle was much larger for smaller particle size, which encouraged disordered crystal orientation on the surface and thus resulted in significantly decreased M_s in smaller nanoparticles. Superparamagnetic nanoparticles quickly respond to the applied external magnetic field, and their remanence and coercivity are negligible. Hence, when superparamagnetic nanoparticles are used in the field of bio, undesirable particle agglomerations originated from the residual magnetism can be avoided. Nanoparticles with superparamagnetic properties have great potential to achieve such desirable properties.

Adsorption process combined with magnetic separation has been used extensively in the processing of minerals and more recently water treatment and environmental application [41]. Magnetite or iron ferrite had been used to separate a wide variety of substances such as dissolved metal species, particulate matter, organic and biological materials. Magnetite has the ability to remove heavy metals as reported by Kochen and Navratil [42] who used a magnetic polymer resin for the removal of actinides and other heavy metals from contaminated water.

In this work, superparamagnetite nanoparticles (MNPs) were synthesized after optimization of conditions and modified subsequently with 3-aminopropyl triethoxysilane and acryloyl chloride. Then the surface of modified nanoparticles was grafted with acrylic acid. The grafted magnetite nanoparticles were next used for separation of heavy metal cations such as Ni^{2+}, Cd^{2+}, Cu^{2+}, Pb^{2+} and the effect of several controling parameters such as residence time, pH and temperature on the separation efficiency was investigated. Also the reproducibility and recovery of adsorbent was checked to show the efficiency of the separation process. The novelties of this work, which might be of more interest are the high potential of such nanoparticles in adsorption of the above heavy metal cations even at very low concentrations and their reproducibilty after several recycling periods.

2. Experimental

2.1. Materials

Ferric chloride hexahydrate ($FeCl_3{\cdot}6H_2O$), ferrous chloride tetrahydrate ($FeCl_2{\cdot}4H_2O$), 3-aminopropyltriethoxysilane (APTES), acryloylchloride (AC), acrylic acid (AA), dichloromethane (DCM), potassium persulphate (KPS), ammonia, copper (II) sulphate, lead (II) nitrate, nickel (II) nitrate, cadmium (II) nitrate, buffer solution (of sodium nitrite with pH 4) were all analytical grade from Merck Chemical Co. They were used without any further purification except for DCM that was dried over P_2O_5 and distilled off. Deionized (DI) water was used in all experiments.

2.2. Equipments

Fourier transform infrared (FT-IR) spectra were recorded on a Bruker FT-IR Tensor27 spectrometer (Germany) with a resolution of 4 cm^{-1}. A small amount of nanoparticle powder was milled with KBr, and the mixture was pressed into a disk for analysis. Thermogravimetric analysis (TGA) was carried out using Pyris TG/DTA (PerkinElmer, USA) thermogravimetric analyzer at a heating rate of 20 °C/min under a flow of nitrogen atmosphere. The essential operations were carried out according to the manufacturer's instructions. The samples were weighed on a Shimadzu LIBRORE AEU-210 analytical electrobalance to an accuracy of 0.0001 g for this analysis. DSC analysis was done by DSC-Netsch (England) With heating rate of 10 °C/min at 50–200 °C under N_2. Size and morphology of the samples were investigated by scanning electron microscopy (SEM) with XL30 instrument from Philips Co. (The Netherlands). 0.1 g of sample was dispersed in 10 ml ethanol in an ultrasound bath and a drop of this dispersion was placed on a sample holder. After evaporation of ethanol, it was placed under vacuum, flushed with Ar, evacuated, and sputter coated with gold sputter coater, SCDOOS (BAL-TEC, Switzerland) for SEM analysis. Magnetite dispersions were prepared in a KERRY Pulsatron

(England) ulterasound bath with frequency of 38 kHz. Magnetic properties of the particles were determined by vibrating sample magnetometer (VSM) PAR-155 (USA). A small amount of sample (powder) was weighed and placed on the probe and the magnetic field was applied in the perpendicular direction to the sample surface. X-ray diffraction (XRD) measurements were carried out with Siemens D-5000 (Germany) using Cu Kα ray (λ = 1.54056 Å) as the radiation source, with a step size of 0.02° and a scan step time of 1 s. The d_{001} basal-spacing of the samples were calculated using the Bragg equation ($d = \lambda/2 \sin\theta$, where λ is the incident wavelength (1.54056 Å) and θ is the diffraction angle [10]). GBC-902/903 atomic spectrophotometer (Spain) was used for determination of cations in the aqueous solutions. The instrument was calibrated in the desired concentration range for each cation (pH 8) to have proper accuracy and precision. These ranges were 7.5–30, 6–25, 0.2–1.8, 2.5–20 ppm for Cu^{2+}, Ni^{2+}, Cd^{2+} and Pb^{2+} respectively.

2.3. Synthesis of magnetite nanoparticles (MNPs)

Magnetite nanoparticles were prepared through coprecipitation method. A solution of $FeCl_3$ and $FeCl_2$ (1:2 molar ratio) was prepared in a three-necked round bottom flask equipped with mechanical stirrer, nitrogen gas inlet and dropping funnel. The ammonia solution was added droppingly while the reaction mixture was stirred at 1200 rpm. After 2 h stirring at 85 °C, the obtained magnetite nanoparticles (black) were magnetically separated, washed with DI water (3 × 25 ml) and ethanol (2 × 30 ml) and then dried under vacuum at 45 °C. The yield of this step was 90.3%.

2.4. Synthesis of modified magnetite with APTES (m-MNPs)

The prepared MNPs were dispersed in ethanol (5 g/l). 25 ml of the above dispersion was diluted with 150 ml ethanol and the dispersing process proceeded with aid of ultrasound bath for 30 min. 4.31 g (19.5 mmol) APTES was added to the above dispersion and stirred for 7 h at room temperature. The product was separated with centrifugation and magnetic field. After washing with ethanol and drying at ambient condition, m-MNPs precipitates were collected with 88.2% yield.

2.5. Preparation of acrylated m-MNPs (m-MNPs-AC)

2 g m-MNPs was dispersed in 10 ml dried DCM and 2 drops of Et_3N was added as the catalyst. A solution of 2 g AC in dried DCM was prepared with 1:10 (v/v) and added to the above dispersion at dropwise 0 °C during 30 min. Then stirring was continued at 0 °C for 2 h. The product was separated magnetically, washed with acetone (5 × 25 ml) and dried under vacuum to give m-MNPs-AC with 79.8%.

2.6. Solution polymerization of AA in the presence of m-MNPs-AC

A three-necked round bottom flask equipped with mechanical stirrer, condenser and nitrogen gas inlet in the water bath was filled with 2.2% m-MNPs-AC, 14.6% AA, 83% DI water and 0.2% KPS. All amounts are in weight percent. The solution polymerization was performed at 70 °C with 500 rpm stirring speed for 6 h. The resulting product (m-PAA) was separated by an external magnetic field, washed with 3 × 25 ml DI water and dried at 45 °C. m-PAA was obtained in 63.5% yield with respect to the added reactants. In the next step, m-PAA was converted to the corresponding sodium salt (m-PAA-Na) with an aqueous solution of NaOH (1.5 M) by increasing the pH of dispersion from 2.5 to 8.5.

2.7. Absorption of heavy metal cations by m-PAA-Na

Four heavy metal cations (Cd^{2+}, Pb^{2+}, Ni^{2+}, Cu^{2+}) were selected for this experiment typically. 1 g m-PAA-Na was dispersed in 10 ml DI water. The above dispersion was added to each standard solution of Cd^{2+}, Pb^{2+}, Ni^{2+} and Cu^{2+} with 1.8, 18, 18, 18 ppm concentration respectively and pH was adjusted at 8 for all of them. The mixture was stirred at 450 rpm and room temperature and the amount of remained cation in the solution was measured by atomic absorption technique after magnetic separation of the m-PAA-Na at different time intervals.

2.8. Evaluation of the absorption capacity after recycling m-PAA-Na

The separated magnetic particles in the above procedure (2.7) were washed with an acidic buffer solution of $NaNO_2$ (pH 4). The washing was continued until no trace of metal cation was observed in the filtrate (measured by atomic absorption). Then the precipitate was dried at 40 °C for 24 h and used again according to the previous section. The weight loss of m-PAA-Na in each step of recycling was about 7.9–12%.

3. Results and discussion

Magnetite nanoparticles were synthesized through coprecipitation method. These nanoparticles have the potential to be surface-modified with functional compounds. Hence, the overall synthetic route has been shown in Scheme 1.

The obtained product can be used as a magnetic cation exchanger polyelectrolyte with the possibility of removal of heavy metal cations as pollutants from aqueous solutions due to their high tendency for dispersion in the aqueous media.

3.1. Synthesis and characterization

Structure of the synthesized compounds (MNPs, m-MNPs, m-MNPs-AC and m-PAA) was characterized by FT-IR spectroscopy (Fig. 1). This technique would be a reliable method for following the variations in the functional groups.

The characteristic peak of magnetite (MNPs) is Fe–O stretching band at 580 cm^{-1} (Fig. 1a). The presence of absorbances at 3415 cm^{-1} (N–H stretching), 1560 cm^{-1} (N–H bending), 2926 cm^{-1} (C–H asymmetrical stretching), 2850 cm^{-1} (symmetrical stretching), 1331 cm^{-1} (C–H bending), 1028 cm^{-1} (Si–O stretching) and 1128 cm^{-1}(C–N stretching) beside characteristic peak of magnetite reveals the progress of condensation reaction between MNPs and APTES (Fig. 1b). FT-IR spectrum of m-MNPs-AC has been shown

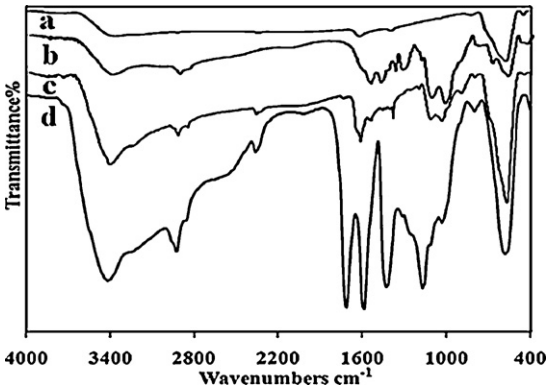

Fig. 1. FTIR spectra of the obtained magnetite nanoparticles (a) MNPs, (b) m-MNPs, (c) m-MNPs-AC and (d) m-PAA.

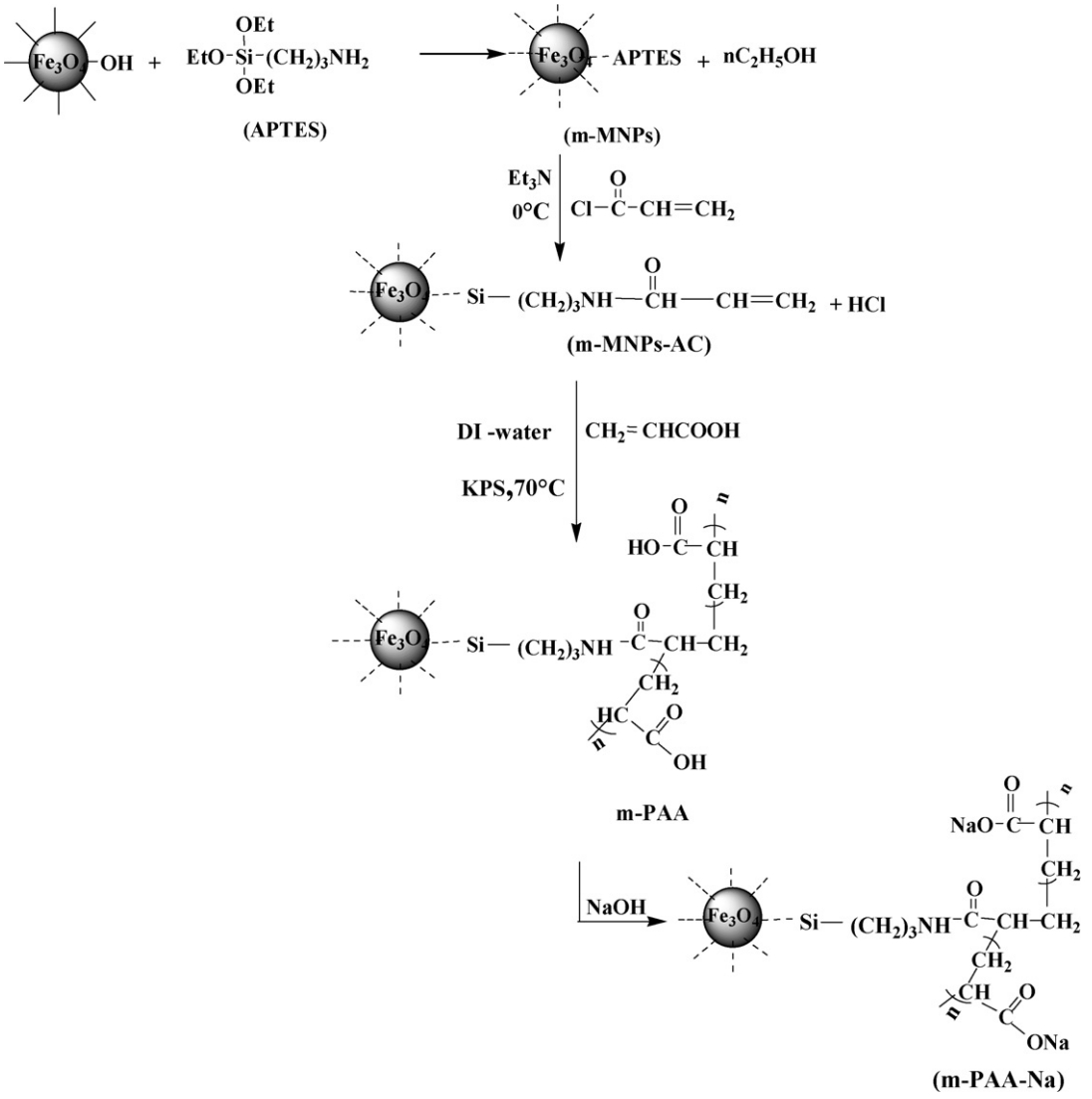

Scheme 1. Preparation of m-PAA-Na-coated magnetite nanoparticle.

in Fig. 1c. Plus to the previous peaks, an absorption has been appeared at 1617 cm^{-1} relating to the amide group stretching band. In m-PAA, the newly formed carboxylic functionalities have been appeared at 1714 cm^{-1}(COO stretching).

XRD analysis was used to investigate the crystalline structure of synthesized MNPs nanoparticles. Six characteristic peaks were observed in the XRD pattern at 2θ of 30.1°, 35.5°, 43.1°, 53.4°, 57.0° and 62.6° (Fig. 2). These are related to the {2 2 0}, {3 1 1}, {4 0 0}, {4 2 2}, {5 1 1} and {4 4 0} planes of Fe_3O_4 spinel structure. It was found that the magnetite crystallites are face-centered cubic, $a = b = c = 8.396$ Å and Fd_3m special group with a size range of 8 nm. The dominant crystal plane is 3 1 1 obtained from Scherrer's equation [43].

The morphology and size of Fe_3O_4 nanoparticles were studied by SEM (Fig. 3). It seems that the particles are semispherical with an average size of 10 nm (determined by a statistical measurement and averaging of 50 particles, with particle size distribution of about 1.28). Their sizes are in correspondence with those obtained from XRD analysis for crystallite structure.

The decrease in particle size will result in the increase in superparamagnetic properties [44–46]. Here, it was tried to optimize the reaction conditions in a way to get the least particle size for obtaining the best magnetic properties. It is noteworthy that the synthetic conditions including type of the base, reaction temperature, stirring speed and time were set in a way to have the desired characteristics for the obtained MNPs.

VSM analysis confirms this claim (Fig. 4). Magnetometery analysis of the synthesized MNPs shows saturation magnetization (M_s) of 57.1 ± 1 emu/g, remanence magnetization (M_r) of 1.8 emu/g and

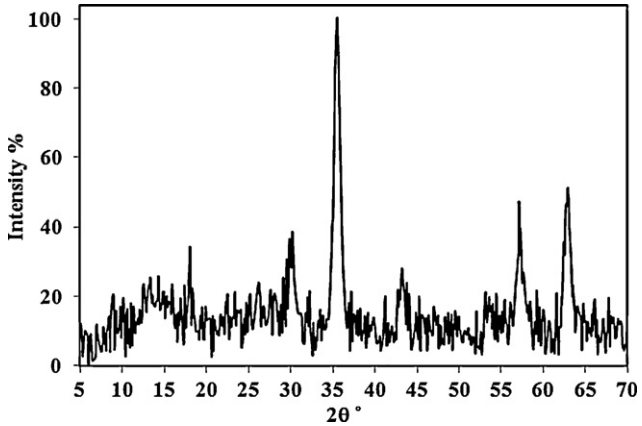

Fig. 2. X-ray powder diffraction pattern of the prepared Fe_3O_4 nanoparticles (MNPs).

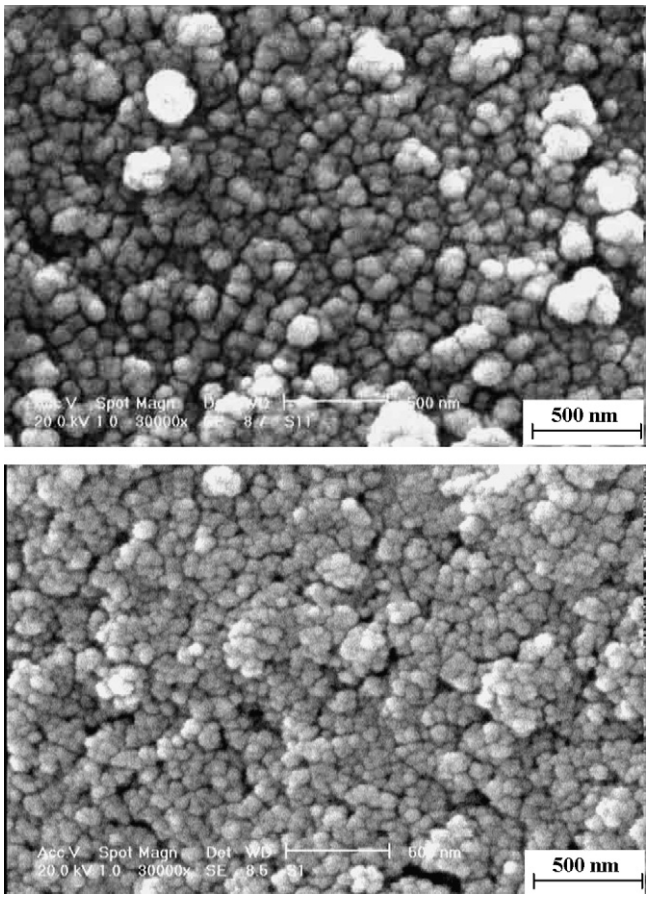

Fig. 3. SEM micrograph of magnetite nanoparticles with semispherical morphology.

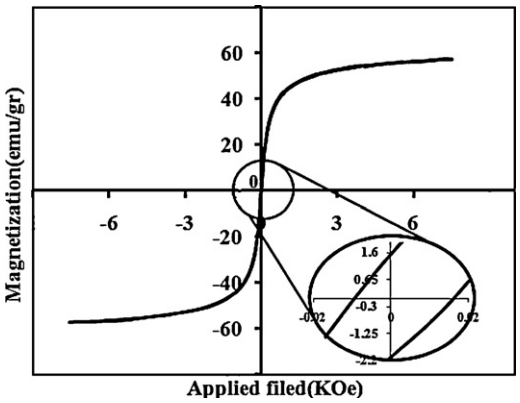

Fig. 4. Magnetization curve of MNPs obtained from VSM analysis at room temperature.

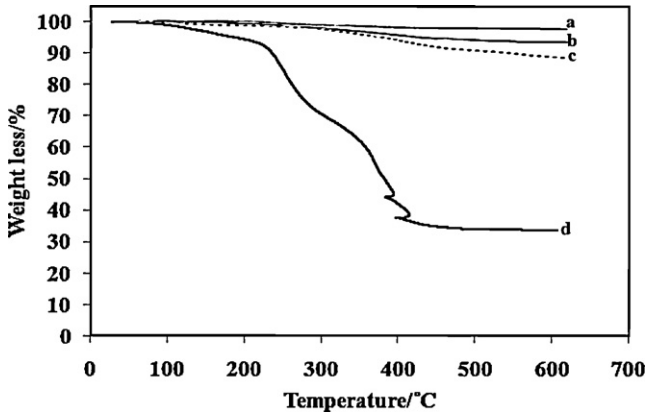

Fig. 5. Thermogravimetric analysis of (a) MNPs, (b) m-MNPs, (c) m-MNPs-AC and (d) m-PAA.

coercivity (H_c) of 12.7 ± 1 Oe. These results prove the preparation of superparamagnetic Fe_3O_4 with $M_r/M_s = 0.031$.

TGA thermograms were used to identify the approximate amounts of modifiers quantatively (Fig. 5). They were carried out up to 600 °C to ensure the removal of organic volatile compounds. The relative comparison between weight loss of each sample with the previous one shows the progress of modification reaction by using the weight percent of residue. The weight loss or extent of modification reaction (relative to the primary MNPs) for m-MNPs, m-MNPs-AC and m-PAA were 6%, 10% and 62%, respectively.

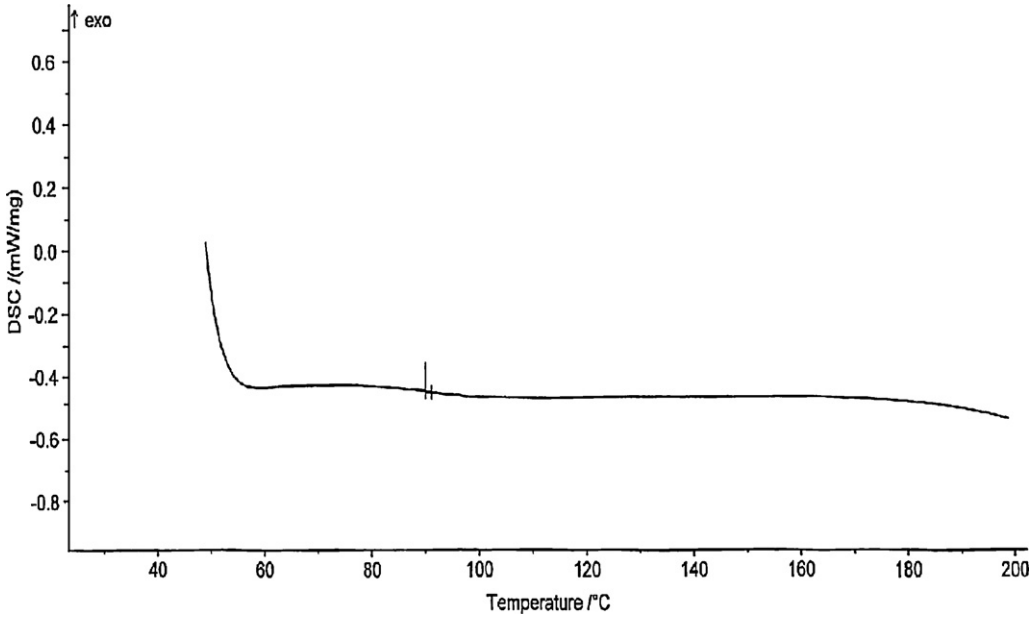

Fig. 6. DSC thermogram of the obtained m-PAA under N_2 atmosphere.

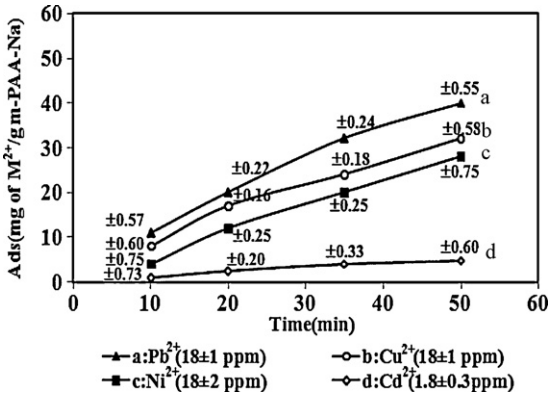

Fig. 7. The changes in adsorption of different cations with residence time at room temperature and pH 8.

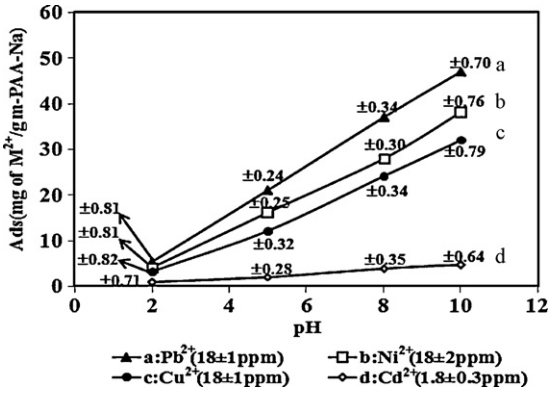

Fig. 8. The effect of pH on the adsorption of heavy metal cations at room temperature (stirring time: 20 min).

These data show that coating and modification of MNPs with polyacrylic acid has been performed successfully and they have been bonded to each other chemically. This is an important result in this work to anchor the polymeric modifier onto the magnetic nanoparticles chemically instead of conventional physical adsorption.

DSC analysis of m-PAA sample shows a glass transition temperature (T_g) at about 90 °C (Fig. 6), which is quite close to the T_g of pure polyacrylic acid (106 °C) [47]. This demonstrates the incorporation and fine dispersion of magnetite nanoparticles into the PAA phase that has reduced the corresponding T_g of homopolymer. This is convenient in organic–inorganic nanocomposite systems as

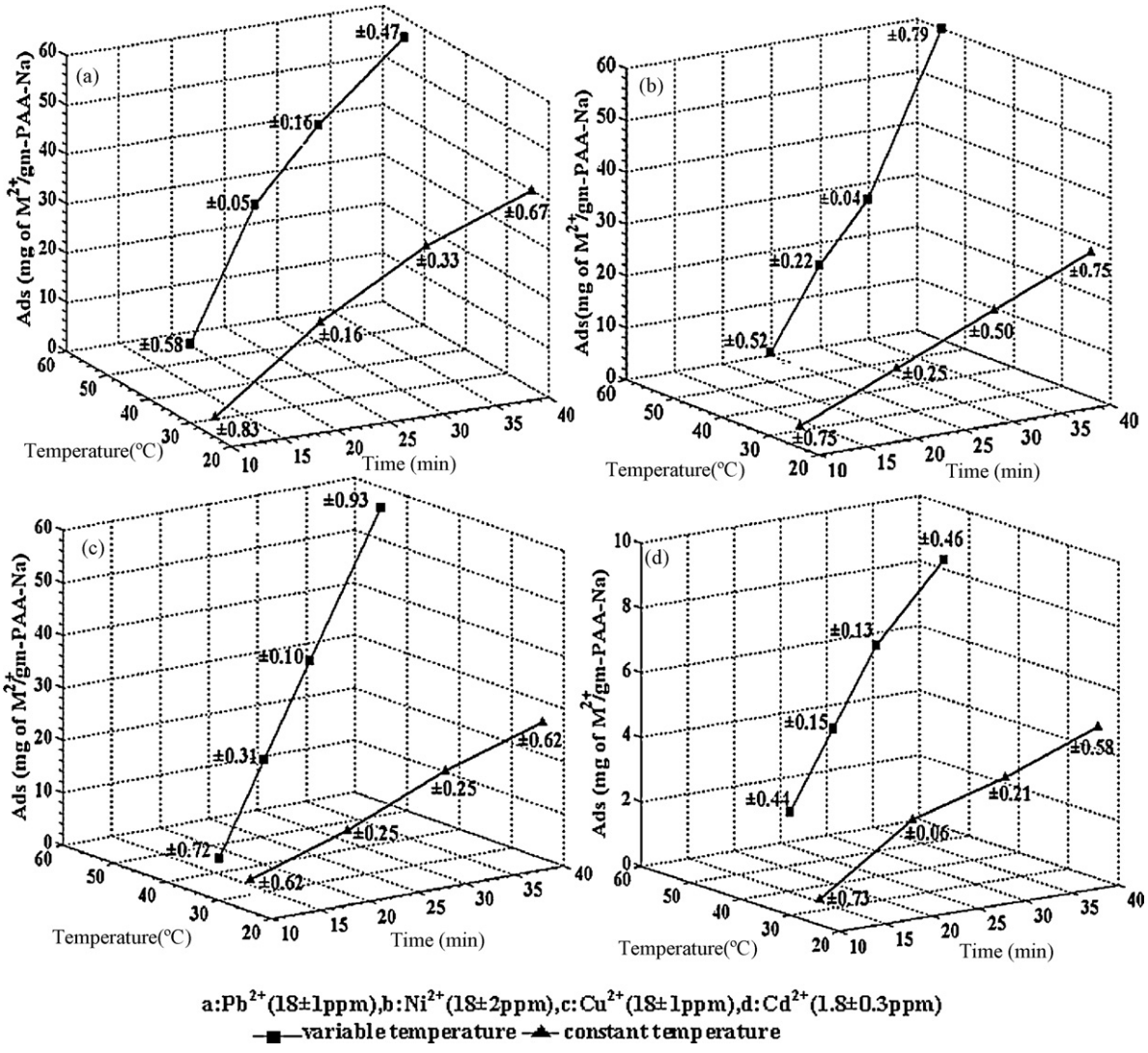

Fig. 9. Adsorption of Ni^{2+}, Cu^{2+}, Cd^{2+} and Pb^{2+} as a function of temperature and residence time (pH 8).

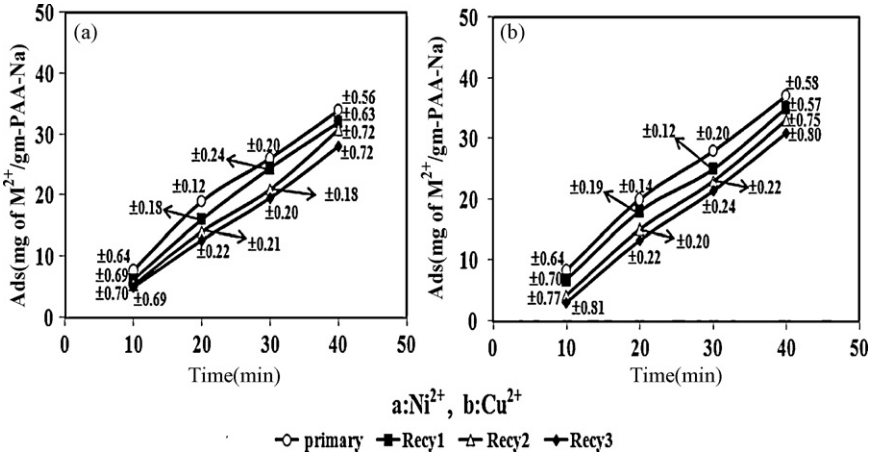

Fig. 10. The changes in adsorption of different cations with residence time and recycled sample (Recy) at room temperature and pH 8. Each number shows the recycling times.

the nanoparticles are present between the polymeric chains and facilitate their segmental motions.

3.2. Separation of heavy metal captions

Four different heavy metal cations, Cu^{2+}, Pb^{2+}, $Ni^{2+}$and Cd^{2+} were chosen for this investigation. These were selected due to their high toxicity in the environment and pollutant effect in the water. So their removal has been a main concern in recent years. The separation procedure was set at low concentration of cations and ease of performance to make it more applicable. For the prepared cation solutions at the constant thermal, time and pH conditions, the maximum adsorption capacity was found to be for Pb^{2+} and the minimum was for Cd^{2+}. These results were obtained from the adsorption curves versus time (Fig. 7). The concentration for each cation was selected as the minimum concentration is the linear region of adsorption. It is notable that the adsorption amount of cations on m-PAA-Na increases with the time and cation concentration in the solution decreases until it is disappeared or removed completely from the solution. This shows the high separation potential and efficiency of the synthesized polymeric-modified magnetite nanoparticles.

The effect of pH of the solutions on cation separation was also investigated (Fig. 8). The pH was regulated to the considered pH in the range of 2–10 by HNO_3 (2.5 M) and NaOH (2 M) solutions. The results show higher chelation tendency of m-PAA-Na at higher pH rather than lower one. This was expectable as at lower pH, the chelation site on m-PAA-Na was occupied with H^+ and they were released at higher pH for originating the desired chelation. It is also worth mentioning that their chelation tendency has linear relationship with the increase in pH.

In another attempt, the effect of temperature on the efficiency of cation adsorption was investigated (Fig. 9). It could be observed that the amount of cation adsorption (by m-PAA-Na) increases with the increase in temperature for all of them and at a constant residence time, the cation separation is improved at higher temperatures. These would be related to the higher mobility of m-PAA-Na chains for performing required chelation due to the more accessibility of the polyelectrolyte chains.

3.3. Reproducibility of cation separation by using of recycled m-PAA-Na

Magnetite-bound polyelectrolytes (m-PAA-Na) were separated after cation adsorption and the chelated cations were released through washing with acidic buffer (pH 4). This was repeated several times to ensure us about the absence of any adsorbed cation by atomic absorption measurement of the filtrate.

The obtained recycled products were used for separation of two cations ($Ni^{2+}$and Cu^{2+}) typically. The results for cation separation have been given for $Ni^{2+}$and Cu^{2+} in Fig. 10.

The procedure was continued after 3 times of recycling and the results reveal that the recycled products have preserved still their capability for separation reasonably. The capacity of cation separation is reduced in about 4–6% during each recycling period and this shows the stability of m-PAA-Na network after separation and recycling procedure. It could be concluded that the chemical bonding between PAA and MNPs plays the major role in retaining the capacity of the m-PAA-Na.

4. Conclusion

Magnetite nanoparticles were prepared by coprecipitation of Fe^{2+} and $Fe^{3+}$with NH_4OH, and then surface-modified with APTES. Scanning electron microscopy shows the average size of 10 nm for magnetite particles and powder X-ray diffraction shows the spinel structure for these nanoparticles. FT-IR spectra indicate that aminosilane molecules have been bound onto the surface of the magnetite nanoparticles through Fe–O–Si chemical bonds. These nanoparticles have the potential to be modified further with functional compounds such as acryloyl chloride. Then they could be used successfully as a magnetic cation exchanger with the possibility of removal of heavy metal cations from water solution through surface polymerization with AA as anionic polyelectrolyte at high pH. The effect of pH, residence time and temperature on cation separation was investigated too. The advantage of this product is its ease of separation by an external magnetic field and possibility of simple recovery after washing with acidic aqueous solution. In addition, efficient adsorption of heavy metal cations (Cd^{2+}, Pb^{2+}, Ni^{2+} and Cu^{2+}) at low concentrations is another benefit of these particles. The capacity of cation separation is reduced in about 4-6% during each recycling step and this shows the stability of m-PAA-Na after separation and recycling process.

References

[1] J. Ying, R.M. Lee, P.S. Williams, J.C. Jeffrey, S.F. Sherif, B. Brian, Z. Maciej, Blood progenitor cell separation from clinical leukapheresis product by magnetic nanoparticle binding and magnetophoresis, Biotech. Bioeng. 96 (2007) 1139–1154.
[2] J. Lee, Y. Jun, S. Yeon, J. Shin, Dual-mode nanoparticle probes for high-performance magnetic resonance and fluorescence imaging of neuroblastoma, J. Cheon Angew. Chem. Int. Ed. 45 (2006) 8160–8162.

[3] N. Tobias, S. Bernhard, H. Heinrich, H. Margarete, V.R. Brigitte, Superparamagnetic nanoparticles for biomedical applications: possibilities and limitations of a new drug delivery system, J. Magn. Magn. Mater. 293 (2005) 483–496.
[4] H. Gu, K. Xu, C. Xu, B. Xu, Biofunctional magnetic nanoparticles for protein separation and pathogen detection, Chem. Commun. 9 (2006) 941–949.
[5] I. Akira, T. Kouji, K. Kazuyoshi, S. Masashige, H. Hiroyuki, M. Kazuhiko, S. Toshiaki, K. Takeshi, Tumor regression by combined immunotherapy and hyperthermia using magnetic nanoparticles in an experimental subcutaneous murine melanoma, Cancer Sci. 94 (2003) 308–313.
[6] B. Steitza, H. Hofmanna, S.W. Kamaub, P.O. Hassab, M.O. Hottigerb, B. Rechenbergc, M. Hofmann-Amtenbrinkd, A. Petri-Fink, Characterization of PEI-coated superparamagnetic iron oxide nanoparticles for transfection: size distribution, colloidal properties and DNA interaction, J. Magn. Magn. Mater. 311 (2007) 300.
[7] X. Hong, J. Li, M. Wang, J. Xu, W. Guo, J.H. Li, Y.B. Bai, T.J. Li, Fabrication of magnetic luminescent nanocomposites using layer-by-layer self-assembly approach, Chem. Mater. 16 (2004) 4022–4027.
[8] S. Wan, J. Huang, M. Guo, H. Zhang, Y. Cao, H. Yan, K. Liu, Biocompatible superparamagnetic iron oxide nanoparticle dispersions stabilized with poly(ethylene glycol)-oligo(aspartic acid) hybrids, J. Biomed. Mater. Res. 80A (2006) 946–954.
[9] R.A. Wassel, B. Grady, R.D. Kopke, K.J. Dormer, Dispersion of superparamagnetic iron oxide nanoparticles in poly(D,L-lactide-co-glycolide) microparticles, Colloid Surf. A: Physicochem. Eng. Aspects 292 (2007) 125–130.
[10] F. Hu, K.G. Neoh, L. Cen, E. Kang, Cellular response to magnetic nanoparticles "PEGylated" via surface-initiated atom transfer radical polymerization, Biomacromolecules 7 (2006) 809–816.
[11] A.M. SchmidtMacromol, The synthesis of magnetic core-shell nanoparticles by surface-initiated ring-opening polymerization of ε-caprolactone, Macromol. Rapid Commun. 26 (2005) 93–97.
[12] X.G. Li, S. Takahashi, K. Watanabe, Y. Kikuchi, M. Koishi, Fabrication and characterististics of Fe_3O_4-polymer composite particles by hybridization, Powder Technol. 133 (2003) 156–163.
[13] H.X. Guo, X.P. Zhao, The synthesis of composite particles responsive to electric and magnetic fields, Opt. Mater. 22 (2003) 39.
[14] G.L. Qiu, Y.L. Li, G.L. Siri, S.Y. Li, Sci. Technol. Chem. Ind. 9 (2001) 15.
[15] E.M. Denkbas, E. Kilicay, C. Birlikseven, E. Ozturk, Magnetic chitosan microspheres: preparation and characterization, React. Funct. Polym. 50 (2002) 225.
[16] S. Sun, S. Anders, H.F. Hamann, J.U. Thiele, J.E.E. Baglin, T. Thomson, E.E. Fullerton, C.B. Murray, B.D. Terris, Polymer mediated self-assembly of magnetic nanoparticles, J. Am. Chem. Soc. 124 (2002) 2884–2885.
[17] A. Kondo, H. Fukuda, Preparation of thermo-sensitive magnetic microspheres and their application to bioprocesses, Colloid Surf. A 153 (1999) 435–438.
[18] A.B. Lowe, B.S. Sumerlin, M.S. Donovan, C.L. Mccormick, Facile preparation of transition metal nanoparticles stabilized by well-defined (co)polymers synthesized via aqueous reversible addition-fragmentation chain transfer polymerization, J. Am. Chem. Soc. 124 (2002) 11562–11563.
[19] K. Ohno, K.M. Koh, Y. Tsujii, T. Fukuda, Synthesis of gold nanoparticles coated with well-defined, high-density polymer brushes by surface-initiated living radical polymerization, Macromolecules 35 (2002) 8989–8993.
[20] N.A. Booker, D. Keir, A. Priestley, C.D. Rithchie, et al., Sewage clarification with magnetite particles, Water Sci. Technol. 23 (1991) 1703–1712.
[21] K.S. Sing, Technology profile, Ground Water Monitor (1994) 60–76.
[22] I. Safarik, M. Safarikova, V. Buricova, Sorption of water soluble organic dyes on magnetic poly(oxy-2, 6-dimethyl-1,4-phenylene, Collect Czech. Chem. Commun. 60 (1995) 1448–1456.
[23] J.D. Orbell, L. Godhino, S.W. Bigger, T.M. Nguyen, et al., Oil spill remediation using magnetic particles: an experiment in environmental technology, J. Chem. Edu. 74 (1997) 1446.
[24] L. Haining, Q. Binju, Y. Xiushen, L. Quan, L. Kangtaek, W. Zhijian, Boron adsorption by composite magnetic particles, Chem. Eng. J. 151 (2009) 235–240.
[25] M. Takafuji, S. Ide, H. Ihara, Z. Xu, Preparation of poly(1-vinylimidazole)-grafted magnetic nanoparticles and their application for removal of metal ions, Chem. Mater. 16 (2004) 1977–1983.
[26] Z. Wu, J. Wu, H. Xiang, M.-S. Chun, K. Lee, Organosilane-functionalized Fe_3O_4 composite particles as effective magnetic assisted adsorbents, Colloid Surf. A 279 (2006) 167–174.
[27] W. Wu, Q. He, C. Jiang, Magnetic iron oxide nanoparticles: synthesis and surface functionalization strategies, Nanoscale Res. Lett. 3 (2008) 397–415.
[28] L.C.A. Oliveira, R.V.R.A. Rios, J.D. Fabris, V. Garg, K. Sapag, R.M. Lago, Activated carbon/iron oxide magnetic composites for the adsorption of contaminants in water, Carbon 40 (2002) 2177–2183.
[29] L.C.A. Oliveira, R.V.R.A. Rios, J.D. Fabris, K. Sapag, Clay–iron oxide magnetic composites for the adsorption of contaminants in water, Appl. Clay Sci. 22 (2003) 169–177.
[30] A. Denizli, R. Say, E. Piskin, Removal of aluminum by Alizarin Yellow attached magnetic poly(2-hydroxyethyl methacrylate) beads, React. Funct. Polym. 55 (2003) 99–107.
[31] D.H. Chen, S.H. Huang, Fast separation of bromelain by polyacrylic acid-bound iron oxide magnetic nanoparticles, Process Biochem. 39 (2004) 2207–2211.
[32] M.H. Liao, D.H. Chen, Preparation and characterization of a novel magnetic nano-adsorbent, J. Mater. Chem. 12 (2002) 3654–3659.
[33] F. Rozada, M. Otero, A. Morán, A.I. García, Adsorption of heavy metals onto sewage sludge-derived materials, Bioresour. Technol. 99 (2008) 6332–6338.
[34] J.P. Chen, W. Wang, Removing copper, zinc and lead ion by granular activated carbon in pretreated fixed-bed columns, Sep. Technol. 19 (2000) 157–167.
[35] Y.F. Shen, J. Tang, Z.H. Nie, Y.D. Wang, Y. Ren, L. Zuo, Preparation and application of magnetic Fe_3O_4 nanoparticles for wastewater purification, Sep. Purif. Technol. 68 (2009) 312–319.
[36] L.H. Cumbal, A.K. Sengupta, Preparation and characterization of magnetically active dual-zone sorbent, Ind. Eng. Chem. Res. 44 (2005) 600–605.
[37] G.D. Moeser, K.A. Roach, W.H. Green, P.E. Laibinis, T.A. Hatton, Water based magnetic fluids as extractants for synthetic organic compounds, Ind. Eng. Chem. Res. 41 (2002) 4739–4749.
[38] S.M. Daliya, R.-S. Juang, An overview of the structure and magnetism of spinel ferrite nanoparticles and their synthesis in microemulsions, Chem. Eng. J. 129 (2007) 51–65.
[39] V.T. Binh, S.T. Purcell, V. Semet, F. Feschet, Nanotips and nanomagnetism, Appl. Surf. Sci. 130–132 (1998) 803–814.
[40] L.C. Varanda, M. Jafelicci Jr., P. Tartaj, K.O. Grady, T. Gonzalez-Carreno, M.P. Morales, T. Munoz, C.J. Serna, Structural and magnetic transformation of monodispersed iron oxide particles in a reducing atmosphere, J. Appl. Phys. 92 (2002) 2079–2085.
[41] J. Davis, Diversity Water Technol., Inc., Chargin Falls, OH, 1997, p. 45.
[42] R.L. Kochen, J.D. Navratil, US Patent 5,955,666 (1997).
[43] B.D. Cullity (Ed.), Elements of X-ray Diffraction, Addison-Wesley, MenloPark, 1978, pp. 123–131.
[44] E.H. Kim, Y. Ahn, H.S. Lee, Biomedical applications of superparamagnetic iron oxide nanoparticles encapsulated within chitosan, J. Alloys Compd. 434–435 (2007) 633–636.
[45] G. Li, Y. Jiang, K. Huang, P. Ding, J. Chen, Preparation and properties of magnetic Fe_3O_4–chitosan nanoparticles, J. Alloys Compd. 466 (2008) 451–456.
[46] Sh. Wang, Y. Zhou, W. Guan, B. Ding, One-step copolymerization modified magnetic nanoparticles via surface chain transfer free radical polymerization, Appl. Surf. Sci. 254 (2008) 5170–5174.
[47] J. Brandrup, E. Immergut, Polymer Handbook, 3rd ed., Wiley-Interscience, U.S., 1989.